Journal of Fluorescence
https://doi.org/10.1007/s10895-024-03634-8

RESEARCH

ZnS:Mn Quantum Dots Coated with a Silica Molecularly Imprinted Polymer for Trace Teflubenzuron Detection in Vegetable Samples

Tian Feng[1] · Zhenkun Chen[1] · Xiaomin Cheng[1]

Received: 10 January 2024 / Accepted: 26 February 2024

Abstract

A novel nanocomposite fluorescent probe consisting of quantum dots and a silica molecularly imprinted polymer (MIPs-capped ZnS:Mn QDs) was synthesized and applied for the rapid detection of teflubenzuron (TBZ) based on the fluorescence quenching of a composite probe via TBZ. The fluorescence quenching efficiency of MIP@SiO2@ZnS:Mn QDs displayed a linear relationship over the concentration range of 0–26.24 μmol/L with a correlation coefficient of 0.9857 and the limit of detection was 2.4 μg/L. The selectivity test showed that the nanocomposite had good selectively rebind TBZ with higher imprinting factor of 3.06 compared with four structurally similar compounds. In addition, the probe was successfully applied to the detection of TBZ in vegetable samples with a recovery of 90.3~97.1% and with a relative standard deviation below 3.2%. This developed method has the advantages of simple preparation, fast response and low toxicity for trace TBZ detection.

Keywords Quantum dots · Molecularly imprinted polymers · Teflubenzuron · Selectively

Introduction

Molecularly imprinted polymers (MIPs) are synthetic receptor-like materials with specific recognition sites for template molecules [1]. The MIPs can rebind the template with high selectivity due to the complementarity of binding sites and template in shape, size and functionality [2]. Therefore, MIPs are used in many applications such as sensors [3–5], solid-phase extraction [6–8] and etc. In particular, the fluorescent properties of fluorescent MIPs have been discovered and used for the detection of analytes with high sensitivity and convenience. A simple method to prepare fluorescent MIPs is to add fluorescent monomers during the synthesis [9], and a few of fluorescent monomers are currently available for direct use [10, 11]. However most of them have to be designed and prepared as new fluorescent monomers for the analytes. QDs are semiconductor nanocrystals that can provide narrow and tunable emission spectra [12]. Compared with traditional organic fluorophores, quantum dots have attracted much attention due to their photochemical stability and good water dispersion. Due to these special properties, quantum dots could be used as fluorescent probes for the efficient detection of trace target molecules.

At present, molecularly imprinted polymers-quantum dots (MIPs-QDs) have attracted much attention due to their unique properties such as their simplicity and efficiency in detecting target molecules [13–17]. Several protocols have been developed to construct the MIPs-based optical materials (QDs). For example, Zhang et al. have composed MIPs-capped CdTe QDs as a sensing material for cytochrome c and demonstrated that the MIPs anchored on the surface of the dBSA modified CdTe QDs could be used as selective materials for recognition of target protein [18]. Li et al. have reported that molecularly imprinted silica nanospm for pyrethroids analysis [19]. Sun et al. proposed a novel fluorescent MIP (SiO_2@CdTe QDs@MIP), which could facilitate an efficient and convenient method for paraquat detection and adsorption [20]. With the trend of environmental protection, the choice of ZnS QDs is becoming increasingly significant due to their low toxicity. There have been several reports on MIPs-ZnS QDs for the detection of pesticides. Zhao et al. successfully prepared composite QDs@MIP nanospheres via a facile and versatile ultrasonication-assisted encapsulation method, which were successfully applied to

Tian Feng and Zhenkun Chen contributed equally to this work.

✉ Xiaomin Cheng
xmcheng@ahu.edu.cn

[1] Key Laboratory Environment-Friendly Polymer Materials of Anhui Province, School of Chemistry and Chemical Engineering, Hefei 230601, China

Published online: 09 March 2024

the fluorescence quantitative detection of diazinon in water [21]. Ren et al. prepared MIPs-capped ZnS:Mn QDs via a sol-gel process, which could be acted as a fluorescence probe and successfully applied to determine nicosulfuron in water samples [22]. In addition, MIPs-QDs have been used for the detection and analysis of pesticide residues such as dimethoate [23], cypermethrin [24], methamidophos [25] and pentachlorophenol [26]. The novel dual-function MIPs-QDs have the advantages of high stability, rapid response, and high sensitivity.

Benzoylurea insecticides (BUs) are common and effective insecticides that poison insects by inhibiting the biosynthesis of chitin in their bodies. BUs have a number of attractive properties, such as high selectivity, good biological activity, rapid degradation in both soil and water, and low acute toxicity for animals [27]. They are widely used on vegetables, fruits and grains, providing a good guarantee of improved crop yields and harvests. However, the excessive use of BUs may lead to serious contamination of agricultural products and potential harm to human health. Therefore, it is great important that the residues of BUs are effectively determined. Some analytical methods have previously been reported on the determination of BUs, such as high performance liquid chromatography (HPLC) [28–30], high performance liquid chromatography with ultraviolet detector [31, 32] and HPLC-mass spectrometry [33–35]. However, these methods encounter hindrances such as expensive equipment, tedious sample pre-treatment or need for highly skilled personnel. Therefore, it is necessary to develop a simple and effective method to recognize and analyse the BUs. To our knowledge, the use of MIPs-QDs to detect BUs residue has not been reported.

In this work, a novel quantum dots-molecularly imprinted polymers (MIPs-capped ZnS:Mn QDs) was prepared by sol-gel using TBZ as a template. The effects of time, pH and template concentration on the fluorescence intensity of MIPs-capped ZnS:Mn QDs were also investigated. Most importantly, four structurally similar compounds were used for selectivity testing to verify the selectivity and recognition ability of MIPs-capped ZnS:Mn QDs. Moreover, the feasibility of MIPs-capped ZnS:Mn QDs materials for the detection of BUs from cabbage samples was examined. This work could provide a new idea for the detection of benzoylurea pesticides.

Materials and Methods

Materials

$ZnSO_4{\cdot}7H_2O$, 3-aminopropyltriethoxysilane (APTES), teflubenzuron (TBZ), diflubenzuron (DBZ) and triflumuron (TFM) were purchased from Aladdin Industrial Corporation. $MnCl_2{\cdot}\ 4H_2O$, sodium hydroxide, hydrochloric acid, methanol, ethanol, acetic acid and ammonia solution (25.0–28.0%) were purchased from Sinopharm Chemical Reagent Co., Ltd (China). 3-Mercaptopropyltriethoxysilane (MPTS) was obtained from Shanghai Macklin Biochemical Co., Ltd. $Na_2S{\cdot}\ 9H_2O$ and tetraethoxysilane (TEOS) were obtained from Tianjin Damao Chemical Reagent Factory. Double distilled water (DDW) was used throughout the experiment. All chemicals were used as received.

Synthesis of ZnS:Mn QDs

ZnS:Mn QDs were synthesized based on the previously reported method [36] and to improve it.12.5 mmol of $ZnSO_4{\cdot}\ 7H_2O$, 0.5 mmol of $MnCl_2{\cdot}\ 4H_2O$, and 40 mL of DDW were placed into a 100 mL three-neck flask, and was ultrasonicated for 10 min under the protection of nitrogen gas. 10 mL aqueous solution with 12.5 mmol $Na_2S{\cdot}\ 9H_2O$ was added dropwise to the mixture, and ultrasonicated continuously for 30 min. Then, 10 mL of an ethanol solution containing 0.625 mmol of MPTS was added, and was ultrasonicated the mixture for 6 h in the dark. Finally, the products ZnS:Mn QDs were collected by centrifugation at 6000 rpm for 20 min and washed with DDW and absolute ethanol three times. The final products were dried at 40 °C under vacuum for 24 h.

Synthesis of MIPs-capped ZnS:Mn QDs

The MIPs-capped ZnS:Mn QDs in this work were prepared according to the reported method [26] with some modifications. Firstly, to a 100 mL flask, 0.1 mmol of TBZ (template) and 0.4 mmol of APTES (functional precursor) were dissolved in 10 mL of absolute ethanol and stirred at room temperature for 30 min. Then 1.0 mL of TEOS was added into the above mixture and continued to stirred for 10 min. After 2.0 mL of 6% ammonia solution and 200 mg ZnS:Mn QDs were added and then stirred for 16 h. Then the resultants were centrifuged at 6000 rpm for 20 min and then washed repeatedly with acetic acid-methanol (1: 9, v/v). The final products were dried at 60 °C under vacuum for 24 h.

As a comparison, NIPs-capped ZnS:Mn QDs were prepared using the same procedure without the addition of TBZ. The synthesis processes of MIPs-capped ZnS:Mn QDs are shown in Fig. 1.

Instruments for Characterization

Fourier transform infrared spectra of prepared composites were recorded by a Nicolet 380 FT-IR spectrometer with the range of 400–4000 cm^{-1}. The XRD spectra were collected on a Smart Lab 9KW with Cu Kα radiation over the 2θ range of 10–70°. The microscopic morphology and surface

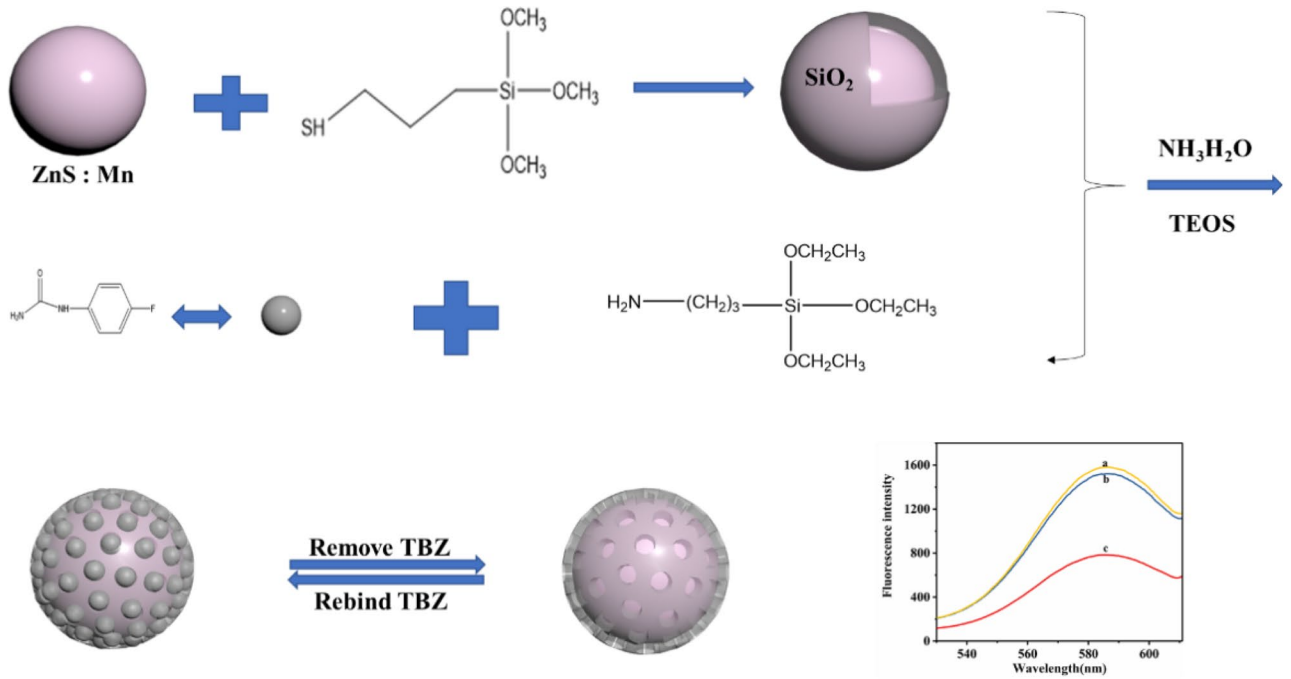

Fig. 1 Schematic representation of the TBZ molecularly imprinted polymer synthesis

structure of the polymers were analysed using a Regulus 8230. Each sample was sputter-coated with a thin layer of gold prior to the SEM measurement. The particle size and size distribution of ZnS:Mn QDs and MIPs-capped ZnS:Mn QDs were determined using a Wyatt Dynapro Nanostar DLS instrument. The measurement time for each sample was 20 s and the results were the mean values of 10 measurements.

Vegetable Sample Preparation

Cabbage samples were purchased from the market. The 5 g sample of chopped and homogenized cabbage juice was mixed with 10 mL of acetonitrile, 3 g of sodium chloride and anhydrous magnesium sulfate. The mixture was shaken and then ultrasonicated for 10 min. The suspension was centrifuged at 6000 rpm for 15 min, and the supernatant was filtered through a 0.22 μm filter membrane. The resulting filtrate was spiked with standard solutions of different concentrations of TBZ and made up to 25 ml with acetonitrile. Then, 500 μL of the real spiked sample was added to a solution containing MIPs-QDs (100 mg/L) at pH 7.0. The concentration of TBZ was calculated by the standard addition method.

Measurement Procedure

All the detections were performed with a Hitachi F-7000 fluorescence spectrophotometer under the same conditions: the slit widths of the excitation and emission were both 10 nm, and the excitation wavelength was set at 320 nm with a recording emission range of 500–615 nm. The photomultiplier tube was set at 600 V. A certain amount of TBZ was dissolved in acetonitrile to get the standard solutions with different concentration (0–100 mg/L). In a 10 mL standard tube, 1 mL of prepared MIPs-QDs suspension (100 mg/L, in DDW) was added and subsequently followed by a given concentration of TBZ solutions, and then mixed thoroughly. The samples were measured with a fluorescence spectrophotometer in several aspects: detection time, detection pH value, liner relationship and selectivity between TBZ and other benzoylureas. The measurement procedure for NIPs-QDs was the same as above.

Results and Discussion

Characterization

The FT-IR spectra of ZnS:Mn QDs, MIPs-QDs and NIPs-QDs were shown in Fig. 2A. The peak at 617 cm^{-1} was attributed to the ZnS band corresponding to sulfuret [37]. From Fig. 2A(1), the peaks appearing at 1118 $cm^{-1}$and 3414 cm^{-1} were caused by Si-O-Si asymmetric stretching vibrations and C-OH stretching vibrations, respectively, which suggested that MPTS was modified on the surface of ZnS:Mn QDs by silylation reaction. Comparing with the spectra of ZnS:Mn QDs, the spectra of MIPs-QDs and NIPs-QDs showed an obvious difference. A new peak appearing

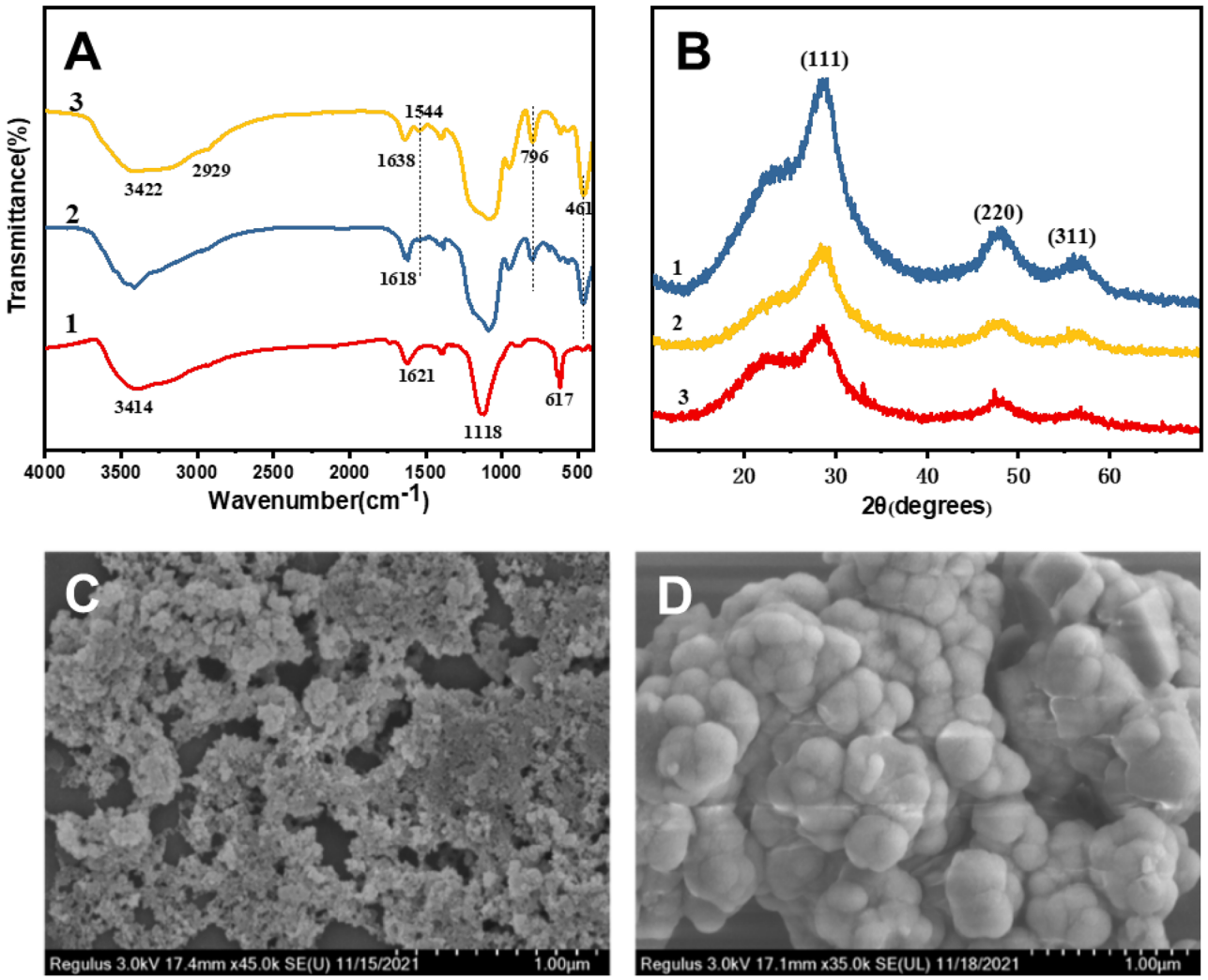

Fig. 2 **A** Fourier transform infrared spectra of ZnS:Mn QDs (1), NIPs-capped ZnS:Mn QDs (2) and MIPs-capped ZnS:Mn QDs (3); **B** X-ray diffraction patterns of ZnS:Mn QDs (1), MIPs-capped ZnS:Mn QDs (2) and NIPs-capped ZnS:Mn QDs (3); SEM images of **C** ZnS:Mn QDs (scale bar: 1 μm) and **D** MIPs-capped ZnS:Mn QDs(scale bar: 1 μm)

at 1544 cm^{-1} was attributed to the N-H bending vibration, indicating the presence of aminopropyl in both MIPs-QDs and NIPs-QDs. The peak of N-H stretching vibration in the spectra of NIPs-QDs was seen at 1618 cm^{-1}, while this peak was shifted to 1638 cm^{-1} in the spectra of MIPs-QDs. Other peaks in the spectra of MIPs-QDs and NIPs-QDs were similar. The peak at 1089 cm^{-1} was assigned to the Si-O-Si asymmetric stretching peak. The peaks at 796 cm^{-1} and 461 cm^{-1} were attributed to Si-O symmetric stretching and Si-O bending vibrations, respectively. These results indicated that the MIPs and NIPs generated from sol-gel condensation of APTES and TEOS was successfully grafted on the surface of MPTS-capped ZnS:Mn QDs.

Figure 2B recorded the X-ray diffraction patterns of MPTS-ZnS:Mn QDs (1), MIPs-QDs (2) and NIPs-QDs (3), and revealed the same diffraction peaks corresponding to the (111), (220) and (311) crystal planes in cubic zinc blende (JCPDS No.65-0309). The results showed that the crystal structure was not changed after the MPTS modification and coating of polymer layer. The ZnS:Mn diffraction peaks of MIPs-QDs and NIPs-QDs became weaker than that of MPTS-ZnS:Mn QDs, which can be explained by the presence of more amorphous phases in MIPs-QDs and NIPs-QDs.

The SEM images of ZnS:Mn QDs and MIPs-QDs were shown in Fig. 2C, D. It can be seen that the particle of ZnS:Mn QDs were small and had uniform size about 16 nm. While the particles of MIPs-QDs were irregularly spherical with a non-uniform size ranging from 150 to 250 nm. The size of ZnS:Mn QDs was smaller than that of MIPs-QDs, and the average particle size of ZnS:Mn QDs and MIPs-QDs in the aqueous solution was measured by dynamic light

scattering (DLS) and the average particle size of ZnS:Mn QDs and MIPs-QDs were estimated at around 16 nm and 185 nm, respectively, the results of DLS were consistent with SEM. These results indicate that MIPs layer has been coated on the surface of QDs.

Stability of the MIPs-QDs and NIPs-QDs

The fluorescence intensities of MIPs-QDs and NIPs-QDs remained relatively constant at 10 min intervals at room temperature over a period of 1 h, as shown in Fig. 3A. This may be due to the fact that the silane layer can effectively protect the polymers and improve its stability. Figure 3B shows the fluorescence intensity at various time when the MIPs-QDs and NIPs-QDs were exposed to TBZ. When a certain amount of TBZ was added, the fluorescence intensity of both MIPs-QDs and NIPs-QDs decreased. The fluorescence intensity of MIPs-QDs was quenched rapidly in the initial 15 min and then became relatively stable, while that of NIPs-QDs decreased rapidly in the first 5 min and then became stable, as show in Fig. 3B. This may be due to the specific interaction between MIPs-QDs and TBZ which caused the fluorescence intensity to be quenched. The results show that the recognition sites of the MIPs-QDs composite can specifically capture the analyte and that the material can be used for rapid and stable determination of TBZ. Hence it was 15 min that was chosen as the optimal time throughout the subsequent experimental.

MIPs-QDs and NIPs-QDs with Different pH and Template (TBZ)

The fluorescence intensity of MIPs-QDs and NIPs-QDs showed great differences with pH values in the presence and absence of TBZ (Fig. 3C). The fluorescence intensity of MIPs-QDs and NIPs-QDs were significantly reduced in the range of pH 5.0–11.0 before the addition of TBZ. After adding TBZ, both MIPs-QDs and NIPs-QDs were obviously quenched, but the fluorescence intensity change of MIPs-QDs composites was greater than that of NIPs-QDs composites. When the pH value was less than 7.0, the fluorescence intensity of the solution was lower, which may be due to the increase of the ionization of H_2S and the increase of the concentration of S^{2-} in the solution, thereby producing ZnS. More ZnS were formed at pH 7.0, resulting in the highest emission fluorescence intensity. As the pH increases from 8 to 11, the fluorescence intensity drops rapidly. The reason is that the silica shell can be ionized at high pH, and OH^- can nucleophilically attack the surface and produce surface defects. The different pH values made larger differences to the fluorescence intensity of MIPs-QDs. So, in order to obtain stable fluorescence intensity and high sensitivity, pH 7.0 was chosen as our further experiment.

Sensitivity of the MIPs-QDs and NIPs-QDs

To further evaluate the recognition and quantitative determination ability of MIPs-QDs, the limit of detection (LOD)

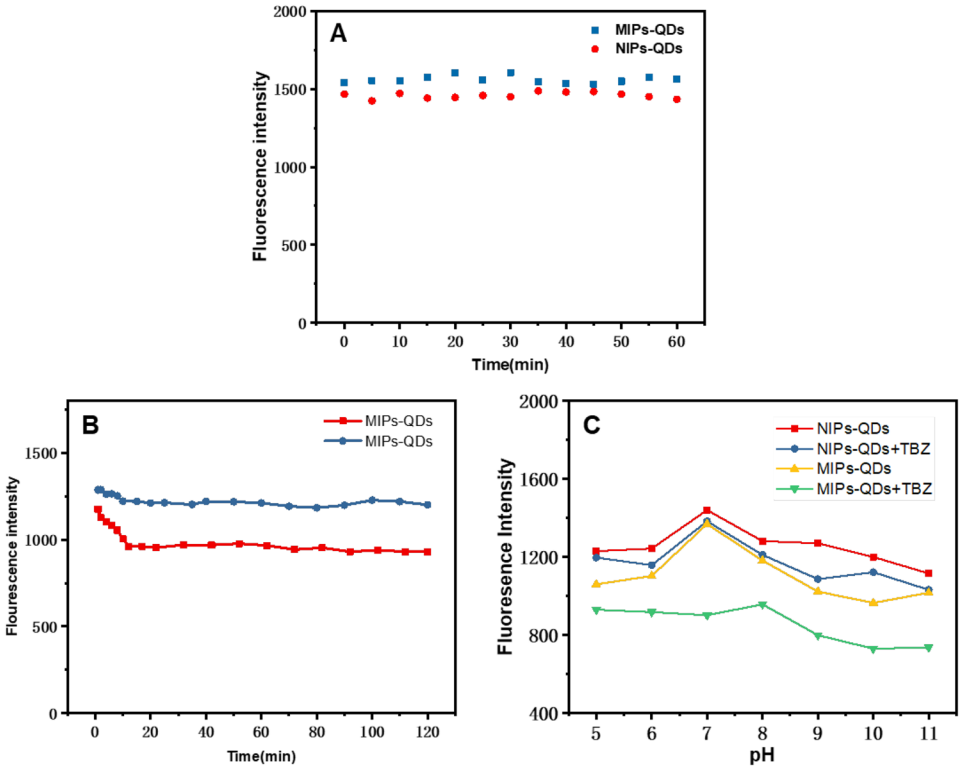

Fig. 3 **A** Influence of time on the fluorescence intensity of MIPs-QDs and NIPs-QDs; **B** Influence of time on the fluorescence quenching between MIPs-QDs and NIPs-QDs and TBZ; **C** The influence of different pH values on the fluorescence intensity of MIPs-capped ZnS:Mn QDs and NIPs-capped ZnS:Mn QDs in the presence and absence of TBZ

and linear range were investigated. The relationship between the fluorescence intensity and the concentration of TBZ can be described by the following formula:

$$F_0/F = 1 + K_{SV}[C] \quad (1)$$

where F_0 and F are the fluorescence intensities in the absence and presence of target molecule, respectively, [C] is the concentration of the TBZ, and K_{SV} is the quenching constant of the quencher. The fitted curve with $R^2 > 0.9857$ reflects a good linear relationship between F_0/F and TBZ.

According to the reported literature, the fluorescent quenching is possibly based on an electron-transfer process [38]. We supposed that the quenching of MIPs-QDs after binding with TBZ was due to the hydrogen bond occurred between the amino groups ($-NH_2$) of the monomer (APTES) and TBZ, which led to the electron transfer from conducting bands of the QDs to the lowest unoccupied molecular orbital of TBZ. The quenching amount is quantitatively related to the concentration of TBZ.

The imprinting factor (IF) was 3.06, indicating that MIPs-QDs had better selectivity than NIPs-QDs. As can be seen from the Fig. 4, the fluorescence intensity decreased with the addition of TBZ, while the fluorescence intensity of NIPs-QDs changes slightly. Thus, the fluorescence of MIPs-QDs was better sensitive compared to NIPs-QDs. This is due to the presence of specific recognition sites in the MIPs-QDs. The detection limit of MIPs-QDs is 2.4 μg/L (calculated by the equation $LOD = 3S_b/K_{SV}$, where S_b was the standard deviation of blank measurement (n = 11) and K_{SV} was the slope of calibration graph).

Selectivity Study

To demonstrate that the obtained MIPs-QDs can selectively adsorb the target molecule even in a mixed system containing other molecules, we performed a selectivity study by comparing the fluorescence intensity response of the MIPs-QDs composites to their template molecule with that to their structural analogue. Four BUs pesticides (hexafiumron, chlorbenzuron, triflumuron and diflubenzuron) were selected as TBZ structural analogues for selective analysis. The linear relationships were showed for BUs of MIPs-QDs and those of NIPs-QDs in Fig. 5A, B, respectively. As shown in Fig. 5A, B, the quantities of changed fluorescence intensity of MIPs-QDs to TBZ was larger than that of the other BUs. At the same time, the changed fluorescence intensity values of NIPs-QDs four BUs were not obvious. This indicates that fluorescence quenching only occurs in the presence of a recognition cavity in the MIPs layer for the template molecule. The specific recognition of TBZ by the prepared MIPs-QDs is attributed to the presence of $-NH_2$ in the APTES, which specifically adsorbs and recognizes TBZ by hydrogen bonding interactions with the template molecule. The experimental results obtained using MIPs-QDs and NIPs-QDs for other BUs pesticides (Table 1) yielded low K_{SV} constants, indicating that the prepared materials are highly selective for the template molecule TBZ. Table 1 also lists imprinting factor (IF) and selectivity factor (SF) which were calculated in accordance with

$$IF = K_{MIP}/K_{NIP} \quad (2)$$

where K_{MIP} and K_{NIP} are the quenching constants of MIPs-QDs or NIPs-QDs with template TBZ, respectively.

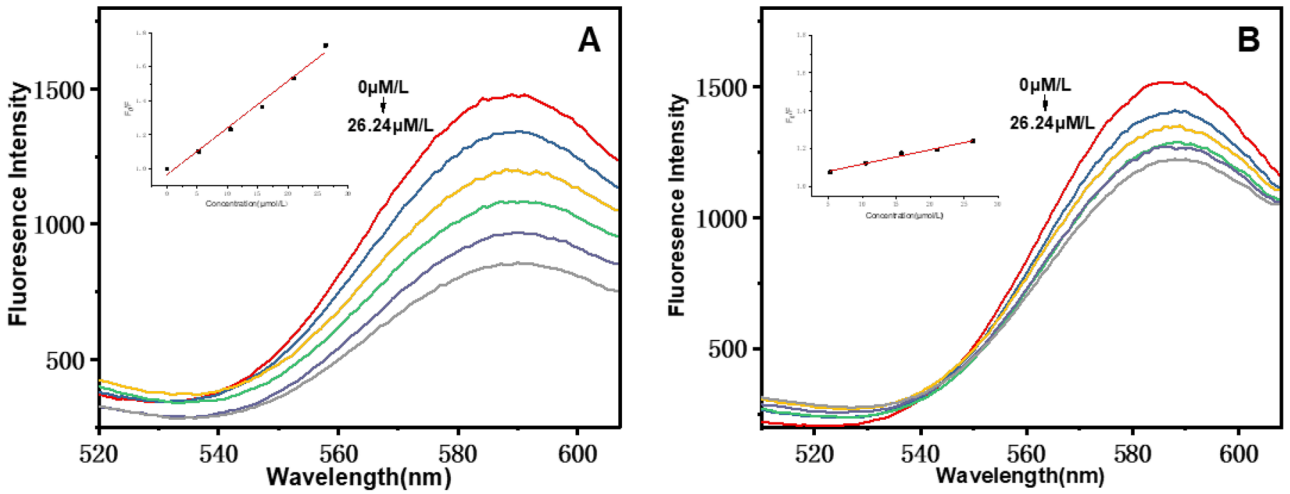

Fig. 4 **A** Fluorescence emission spectra of MIPs-ZnS:Mn QDs; **B** NIPs-ZnS:Mn QDs

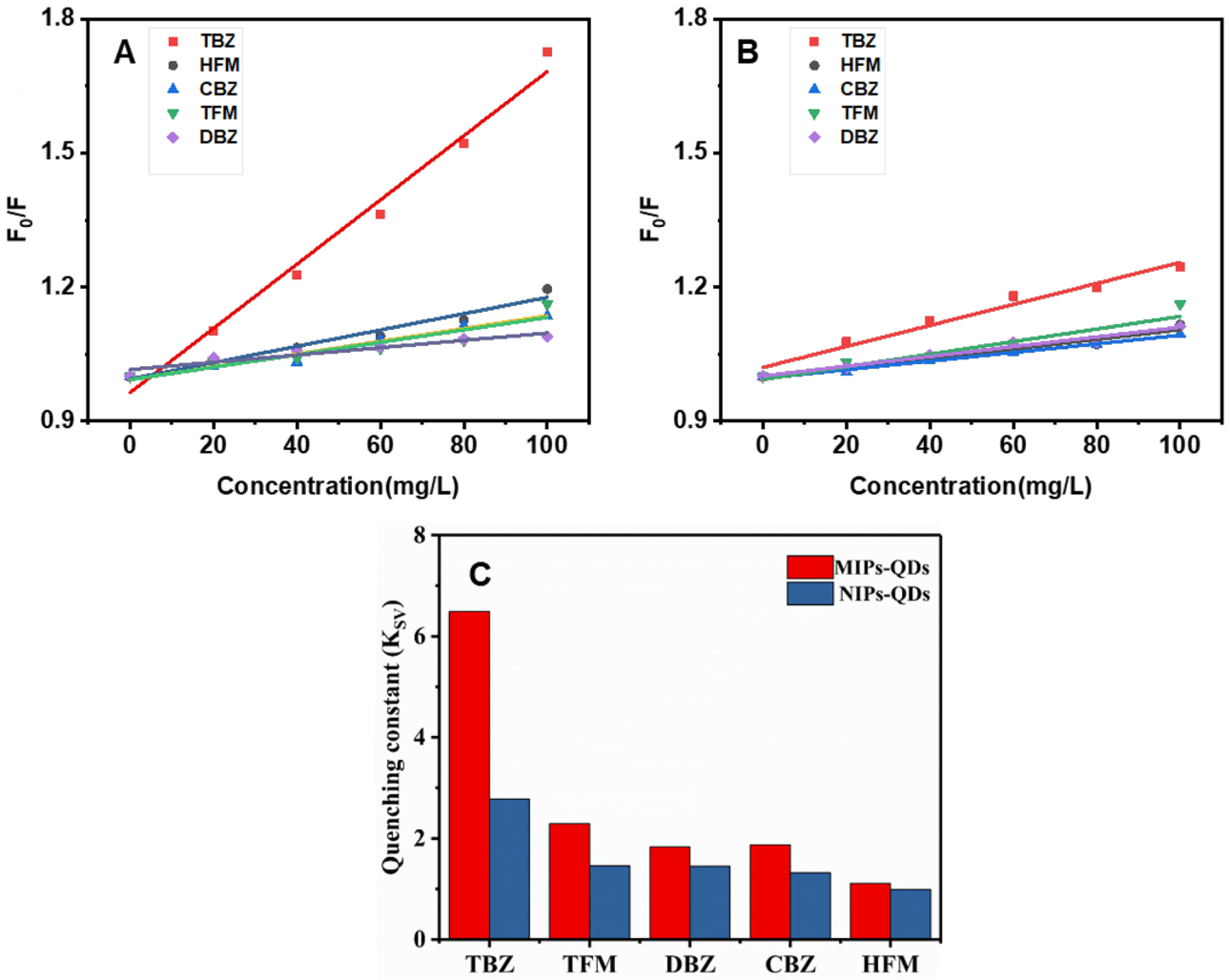

Fig. 5 **A** Quenching constant of MIPs-capped ZnS:Mn QDs by different kinds of benzoylureas at pH 7.0; **B** Quenching constant of NIPs-capped ZnS:Mn QDs by different kinds of benzoylureas at pH 7.0; **C** The imprinting factors of MIPs-and NIPs-capped ZnS:Mn QDs for standard solutions of five benzoylurea insecticides

$$SF = K_{MIP}(target)/K_{MIP}(non\text{-}target) \quad (3)$$

where K_{MIP}(target) is the quenching constants of MIPs-QDs with template TBZ, and K_{MIP}(non-target) is the quenching constants of MIPs-QDs with others. IF was used to evaluate the recognition ability of the MIPs-QDs by monitoring the fluorescence. The selectivity of the MIPs for the target molecule increases as the IF value increases. The SF is usually considered as a better determinant of selectivity. As shown in Table 1, for the TBZ the IF values and were much higher than for the other BUs and the SF values were 3.92, 5.06, 5.17 and 8.76 respectively. These results indicated that the synthetic MIPs-QDs had higher recognition ability for TBZ than other BUs. In addition, the extent of TBZ quenching did not show any significant specificity of NIPs-QDs compared with other BUs insecticides. This phenomenon can be reasonably explained by the fact that specific recognition sites complementary to TBZ in shape, size and spatial arrangement were generated on the surface of the MIPs-QDs during the synthesis process. The results indicated that MIPs-QDs were better specific to TBZ but less specific to other BUs.

Table 1 Stern-Volmer constants, imprinting effect, and selectivity factors for TBZ and other BUs

	K_{SV}(MIP)	K_{SV}(NIP)	IF	SF
TBZ	0.00718	0.00235	3.06	\
HFM	0.00183	0.00109	1.68	3.92
CBZ	0.00142	0.00097	1.46	5.06
TFM	0.00139	0.00141	0.99	5.17
DBZ	0.00082	0.00109	0.75	8.76

Table 2 Recovery of TBZ in real samples with TBZ solution at different concentration

Cabbage juice samples	TBZ spiked(mg/L)	Found(mg/L)	Recovery(%)	RSD(n = 3,%)
1	1.00	0.9504	95.0	2.8
2	3.00	2.7104	90.4	3.2
3	5.00	4.8544	97.1	2.5

Table 3 Comparison between the MIPs-QDs and other methods for the detection of TBZ

Methods	Samples	LOD(μg/L)	Recovery(%)	RSD(%)	Reference
DLLME-HPLC	White grape juice	6.2	89.5–95.4	1.6–4.6	[39]
SPE-HPLC	Peer juice drink	13.6	81.3–85.2	1.7	[40]
MSPE-HPLC/MOFs	Fruit juice	0.5	80.9–89.1	3.8–6.5	[41]
MSPE-HPLC/MOFs	Environment water	1.5	89.6–74.4	0.9–7.2	[42]
MIPs-QDs	Cabbage juice	2.4	90.4–97.1	2.5–3.2	This work

Application to Vegetable Samples Analysis

In order to verify the feasibility of the MIPs-QDs analysis for real samples, the cabbage juice samples spiked at different concentrations of TBZ were determined by using the proposed method. They were applied to determine the TBZ of spiking cabbage juice samples. As was shown in Table 2, the recovery study was carried out on the samples spiked with 1.0–5.0 mg/L TBZ to evaluate the developed the composites, and the corresponding results were listed judge the accuracy of this method. The average recoveries from samples were varied between 90.35% to 97.09% with relative standard deviations (RSD) in the range of 2.45–3.17%. The presence of specific recognition sites in MIPs-QDs has a high recovery effect on TBZ. Thus, the developed MIPs-QDs can be used detect TBZ in real sample.

The comparison between the MIPs-QDs and other methods for the detection of TBZ is shown in Table 3. As can be seen, the MIPs-QDs showed relatively excellent levels of recovery and RSD. However, the LOD is higher than MSPE-HPLC/MOFs method. In comparison to chromatographic methods, fluorescence technology is used instead of tedious chromatographic separation process, resulting in saved analysis time. Furthermore, our method is simple and rapid compared to other methods. Meanwhile, the materials used in this method are highly selective because of using molecularly imprinting technique. However, while retaining the high selectivity of the MIPs-QDs system, we need to further improve the sensitivity of the system.

Conclusions

In this study, we have developed a novel strategy to fabricate the core-shell spherical silica molecularly imprinted polymer based on ZnS:Mn QDs for the detection of teflubenzuron. The nanocomposites were prepared and characterized by FT-IR, SEM, DLS, FL and XRD. The binding time, pH value of the solution and different concentrations of TBZ played important roles on the binding ability. Under optimal conditions, the MIPs-capped ZnS:Mn QDs was applied to detection of TBZ based on the fluorescence quenching with a higher imprinting factor. The detection of teflubenzuron in real sample was successfully carried out with good recoveries and a very low detection limit. This work would provide a method with a promising potential for the on-site detection of TBZ residues in real samples or in environmental waters.

Author Contributions T.F. and Z.C., investigation, methodology, and writing original draft, X.C., supervision, project administration, and review & editing.

Funding None.

Data Availability No datasets were generated or analysed during the current study.

Declarations

Ethical Approval Not applicable.

Competing Interests The authors declare no competing interests.

References

1. Huang DL, Wang RZ, Liu YG, Zeng GM, Lai C, Xu P, Lu BA, Xu JJ, Wang C, Huang C (2014) Application of molecularly imprinted polymers in wastewater treatment: a review. Environ Sci Pollut Res 22:963–977. https://doi.org/10.1007/s11356-014-3599-8
2. Zheng L, Wang H, Cheng X (2018) Molecularly imprinted polymer nanocarriers for recognition and sustained release of

diclofenac. Polym Adv Technol 29:1360–1371. https://doi.org/10.1002/pat.4247
3. Kotova K, Hussain M, Mustafa G, Lieberzeit PA (2013) MIP sensors on the way to biotech applications: targeting selectivity. Sens Actuators B Chem 189:199–202. https://doi.org/10.1016/j.snb.2013.03.040
4. Iqbal N, Mustafa G, Rehman A, Biedermann A, Najafi B, Lieberzeit AP, Dickert LF (2010) QCM-arrays for sensing terpenes in fresh and dried herbs via bio-mimetic MIP layers. Sensors 10(7):6361–6376. https://doi.org/10.3390/s100706361
5. Pérez -Moral N, Mayes AG (2006) Direct rapid synthesis of MIP beads in SPE cartridges. Biosens Bioelectron 21(9):1798–1803. https://doi.org/10.1016/j.bios.2005.08.014
6. Alves L, Erbetta C, Fernandes C (2015) Synthesis and characterization of MIP with phenylalanine for their application in SPE. Polímeros 25(6):596–605. https://doi.org/10.1590/0104-1428.2116
7. Lu YQ, Lin Z, Wei F, Tw T (2007) Evaluation of the polymerization and recognition mechanism for phenol imprinting SPE. Chromatographia 66(5–6):339–347. https://doi.org/10.1365/s10337-007-0336-1
8. Say R, Erdem M, Ers ZA, Turk H, Denizli A (2005) Biomimetic catalysis of an organophosphate by molecularly surface imprinted polymers. Appl Catal A 286(2):221–225. https://doi.org/10.1016/j.apcata.2005.03.015
9. Zhou TC, Halder A, Sun Y (2018) Fluorescent nanosensor based on molecularly imprinted polymers coated on graphene quantum dots for fast detection of antibiotics. Biosensors 8(3):82. https://doi.org/10.3390/bios8030082
10. Mark VS, William JS, Philippa CH, Tim M, Subrayal MR (2021) Green synthesis as a simple and rapid route to protein modified magnetic nanoparticles for use in the development of a fluorometric molecularly imprinted polymer-based assay for detection of myoglobin. Nanotechnology 32(9):095502. https://doi.org/10.1088/1361-6528/abce2d
11. Yadiris G, Joanna C, Eduardo DP, Sergey AP, Elema P (2021) A magnetic molecularly imprinted nanoparticle assay (MINA) for detection of pepsin. React Funct Polym 170:105133. https://doi.org/10.1016/j.reactfunctpolym.2021.105133
12. Yang YQ, Yi CL, Luo J, Liu R, Liu JK, Jiang JQ, Liu XY (2011) Glucose sensors based on electrodeposition of molecularly imprinted polymeric micelles: a novel strategy for MIP sensors. Biosens Bioelectron 26(5):2607–2612. https://doi.org/10.1016/j.bios.2010.11.015
13. Yang Y, Niu H, Zhang H (2016) Direct and highly selective drug optosensing in real, undiluted biological samples with quantum-dot-labeled hydrophilic molecularly imprinted polymer microparticles. ACS Appl Mater Interfaces 8:15741–15749. https://doi.org/10.1021/acsami.6b04176
14. Panagiotopoulou M, Kunath S, Medina-Rangel PX, Haupt K, Bui BTS (2017) Fluorescent molecularly imprinted polymers as plastic antibodies for selective labeling and imaging of hyaluronan and sialic acid on fixed and living cells. Biosens Bioelectron 88:85–93. https://doi.org/10.1016/j.bios.2016.07.080
15. Li CY, Yang Q, Wang XY, Arabi M, Peng H, Li JH, Xiong H, Chen LX (2020) Facile approach to the synthesis of molecularly imprinted ratiometric fluorescence nanosensor for the visual detection of folic acid. Food Chem 319:126575. https://doi.org/10.1016/j.foodchem.2020.126575
16. Yang Y, Chang Y, Guo Y, Yu L, Zhang G, Zhai D, Wang XM, Sun XT (2019) Fluorometric microplate-based dimethoate assay using CdSe/ZnS quantum dots coated with a molecularly imprinted polymer. Microchimica Acta 186(8):1–10. https://doi.org/10.1007/s00604-019-3649-5
17. Shirani MP, Rezaei B, Ensafi A, Ramezani AM (2020) Development of an eco-friendly fluorescence nanosensor based on molecularly imprinted polymer on silica-carbon quantum dot for the rapid indoxacarb detection. Food Chem 339(11):127920. https://doi.org/10.1016/j.foodchem.2020.127920
18. Wei Z, Xi-W H, Yang C, Li WY, Zhang YK (2011) Composite of CdTe quantum dots and molecularly imprinted polymer as a sensing material for cytochrome c. Biosens Bioelectron 26(5):2553–2558. https://doi.org/10.1016/j.bios.2010.11.004
19. Haibing L, Yuling L, Jing C (2010) Molecularly imprinted silica nanospheres embedded cdse quantum dots for highly selective and sensitive optosensing of pyrethroids. Chem Mater 22(8):2451–2457. https://doi.org/10.1021/cm902856y
20. Sun J, Chen C, Zhang Y, Sun XL (2020) A novel fluorescent molecularly imprinted polymer SiO2@CdTe QDs@MIP for paraquat detection and adsorption. Luminescence 36:345–352. https://doi.org/10.1002/bio.3949
21. Zhao Y, Ma Y, Li H, Wang LY (2012) Composite QDs@MIP nanospheres for specific recognition and direct fluorescent quantification of pesticides in aqueous media. Anal Chem 84(1):386–395. https://doi.org/10.1021/ac202735v
22. Ren X, Chen L (2015) Preparation of molecularly imprinted polymer coated quantum dots to detect nicosulfuron in water samples. Anal Bioanal Chem 407(26):8087–8095. https://doi.org/10.1007/s00216-015-8982-x
23. Behrouz V (2017) Specific fluorescence probe for direct recognition of dimethoate using molecularly imprinting polymer on ZnO quantum dots. J Fluoresc 27(4):1–9. https://doi.org/10.1007/s10895-017-2068-4
24. Ren X, Chen L (2015) Quantum dots coated with molecularly imprinted polymer as fluorescence probe for detection of cyphenothrin. Biosens Bioelectron 64:182–188. https://doi.org/10.1016/j.bios.2014.08.086
25. Liu XY, Liu QR, Kong XG, Qiao XG, Xu ZX (2017) Molecularly imprinted fluorescent probe based on hydrophobic CdSe/ZnS quantum dots for the detection of methamidophos in fruit and vegetables. Adv Polym Technol 37(6):1790–1796. https://doi.org/10.1002/adv.21838
26. Wang HF, He Y, Ji TR, Yan XP (2009) Surface molecular imprinting on Mn-doped ZnS quantum dots for room-temperature phosphorescence optosensing of pentachlorophenol in water. Anal Chem 81(4):1615–1621. https://doi.org/10.1021/ac802375a
27. Kamal KJ, Elena PV, Pilar BB, Antonio MP (2020) Synthesis and application of a surface ionic imprinting polymer on silica-coated Mn-doped ZnS quantum dots as a chemosensor for the selective quantification of inorganic arsenic in fish. Anal Bioanal Chem 412(7):1663–1673. https://doi.org/10.1007/s00216-020-02405-1
28. Sun R, Liu C, Zhang H (2015) Benzoylurea chitin synthesis inhibitors. J Agric Food Chem 63(31):6847–6865. https://doi.org/10.1021/acs.jafc.5b02460
29. Wang CH, Ma XX, Wang C, Wu QH, Wang Z (2014) Poly (vinylidene fluoride) membrane based thin film microextraction for enrichment of benzoylurea insecticides from water samples followed by their determination with HPLC. Chin Chem Lett 25(12):1625–1629. https://doi.org/10.1016/j.cclet.2014.06.018
30. Martínez-Galera M, López-López T, Gil-García MD, Martinez-vidal JL, Vazquez PP (2001) Determination of benzoylureas in tomato by high-performance liquid chromatography using continuous on-line post-elution photoirradiation with fluorescence detection. J Chromatogr A 918(1):79–85. https://doi.org/10.1016/S0021-9673(01)00653-7
31. Duo H, Li Y, Liang X, Wang S, Wang LC, Gou Y (2020) Magnetic 3D hierarchical Ni/Nio@C nanorods derived from metal-organic frameworks for extraction of benzoylurea insecticides prior to HPLC-UV analysis. Microchim Acta 187(1):88. https://doi.org/10.1007/s00604-019-4013-5
32. Likas DT, Tsiropoulos NG (2009) Residue screening in apple, grape and wine food samples for seven new pesticides using HPLC with UV detection. An application to trifloxystrobin dissipation

in grape and wine. Int J Environ Anal Chem 89(8–12):857–869. https://doi.org/10.1080/03067310902756615
33. Han X, Lou XS, Zhang L, Wang GQ, Ma M, Wang ML (2010) Determination of benzoylurea and bishydrazide pesticide residues in vegetables by ultra performance liquid chromatography-tandem mass spectrometry with matrix solid phase dispersion. Chin J Chromatogr 28(4):341–347. https://doi.org/10.3724/SP.J.1123.2010.00341
34. Lian-Feng AI, Wang FC, Chen RC (2010) Rapid HPLC-MS/MS determination of residual amounts of 7 benzoylurea insecticides in fruits. Phys Testing Chem Anal 46:1001–4020. https://doi.org/10.1360/972010-874
35. Chen L, Chen J, Guo Y, Li J, Yang Y, Xu L, Fu F (2014) Study on the simultaneous determination of seven benzoylurea pesticides in Oolong tea and their leaching characteristics during infusing process by HPLC-MS/MS. Food Chem 143:405–410. https://doi.org/10.1016/j.foodchem.2013.08.027
36. Zhou CY, Song JH, Zhou LY, Zhong LP, Liu JX, Qi YY (2015) Greener synthesis and optimization of highly photoluminescence Mn2+-doped ZnS quantum dots. J Lumin 158:176–180. https://doi.org/10.1016/j.jlumin.2014.09.053
37. He Y, Wang HF, Yan XP (2008) Exploring Mn-doped ZnS quantum dots for the room-temperature phosphorescence detection of enoxacin in biological fluids. Anal Chem 80(10):3832–3837. https://doi.org/10.1021/ac800100y
38. Zhang L, Chen L (2018) Visual detection of melamine by using a ratiometric fluorescent probe consisting of a red emitting CdTe core and a green emitting CdTe shell coated with a molecularly imprinted polymer. Microchim Acta 185:135–143. https://doi.org/10.1007/s00604-017-2664-7
39. Zhou JK, Han CJ, Tang CL, Fu YF (2013) Determination of benzoylurea insecticides in white grape juice by high performance liquid chromatography. Food Sci 34(10):169–172. https://doi.org/10.7506/spkx1002-6630-201310036
40. Zhou JK, Yang DX, Xu P (2011) Determination of benzoylurea insecticides in pear juice drink by salting out phase separation solid phase extraction-high performance liquid chromatography. Food Sci Technol 36(8):309–311. https://doi.org/10.13684/j.cnki.spkj.2011.08.078
41. Duo H, Lu X, Wang S, Wang L, Guo Y, Liang X (2019) Synthesis of magnetic metal-organic framework composites, Fe_3O_4-NH_2@MOF-235, for the magnetic solid-phase extraction of benzoylurea insecticides from honey, fruit juice and tap water samples. New J Chem 43:12563–12569. https://doi.org/10.1039/C9NJ01988J
42. Niu M, Li Z, Zhang S, He W, Li J, Lu R, Gao H, Zeng A, Zhou W (2020) Hybridization of metal-organic frameworks with attapulgite for magnetic solid phase extraction and determination of benzoylurea insecticides in environmental water samples. Microchem J 159:105392. https://doi.org/10.1016/j.microc.2020.105392